

Traversable Wormholes in a viable $f(R)$ Gravity Model

Anshuman Baruah^{*}, Parangam Goswami, and Atri Deshamukhya

Department of Physics, Assam University, Silchar, Assam, India-788011

Abstract

Traversable wormhole solutions in general relativity (GR) require *exotic* matter sources that violate the null energy condition. $f(R)$ gravity has been studied extensively as a viable alternative to GR, and traversable wormhole solutions in $f(R)$ gravity have been discussed extensively. In this study, we analyze the energy conditions for spherically symmetric traversable Morris-Thorne wormholes in a recently proposed viable $f(R)$ gravity model. We analyze wormhole space-times considering both constant and variable redshift functions, and demonstrate that traversable wormholes can be realized in this theory with minimal or no violations of the null energy condition with suitable choices of model and metric parameters.

1 Introduction

Wormholes are compact regions of space-time with topologically simple boundaries and topologically non-trivial interiors [1]. They are solutions to the Einstein's field equation (EFE) of general relativity (GR), describing two asymptotically flat regions of space-time connected by a 'throat'. Both asymptotically flat surfaces may be separated by arbitrarily large distances. Stable wormhole solutions can be formulated in GR [2] at the expense of violating the null energy condition (NEC), which ensures that the observed energy density of matter fields in the EFEs is positive for any observer. Traversable wormholes in GR can be described by the following line element [2] :

$$ds^2 = -e^{2\Phi(r)} dt^2 + \frac{dr^2}{1 - \frac{b(r)}{r}} + r^2 d\theta^2 + r^2 \sin^2 \theta d\phi^2, \quad (1)$$

where $\Phi(r)$ determines the gravitational redshift, and is called the redshift function; and $b(r)$ determines the spatial shape of the wormhole, and is called the wormhole shape function. Traversable wormholes allow signals that fall in one asymptotically flat region to emerge through the throat (located at some $r = r_0$) in the other asymptotically flat region. In order for the wormhole described by Eq. (1) to be traversable, the following constraints are imposed on the metric functions $\Phi(r)$ and $b(r)$. Firstly, event horizons are not allowed in wormhole space-times. Horizons in spherically symmetric space-times are identified by physically non-singular surfaces at $g_{00} = -e^{2\Phi} \rightarrow 0$. Thus, we impose the constraint that $\Phi(r)$ must be finite everywhere throughout the space-time. Secondly, the throat of the wormhole is located at some minimum radius $r = r_0$, where $b(r_0) = r_0$. Since the corresponding metric component is singular at the throat, the proper distance $l(r)$ must be well-behaved.

$$l(r) = \pm \int_{r_0}^r \frac{dr}{\sqrt{1 - b(r)/r}} \quad (2)$$

Therefore, the above integral must be regular throughout the space-time, which requires that $1 - b(r)/r \geq 0$. Moreover, $b(r)$ should satisfy the *flaring-out* condition [2] given by $(b(r) - b'(r)r)/b^2 > 0$. These constraints on the metric functions impose constraints via the EFEs on the mass-energy density and radial and lateral pressures of the matter that threads the geometry, which lead to violations of various energy conditions [2]. The matter source threading such wormholes is conventionally described by an anisotropic perfect fluid with a diagonal stress-energy tensor, $T_{\mu\nu} = \text{diag}(\rho, p_r, p_t, p_t)$, where ρ is the energy density, p_r is the radial pressure, and p_t is the lateral pressure. The NEC requires that $\rho + p_r \geq 0$, whereas wormholes in GR require that $\rho + p_r < 0$ for matter sources threading

^{*}E-mail: anshuman.baruah@aus.ac.in

wormhole space-times [2]. Moreover, this leads to the violation of the weak energy condition (WEC), $\rho \geq 0$, and matter sources with these properties are referred to as *exotic*. Such behavior is considered exotic mainly because negative energy densities ($\rho < 0$) have never been observed (with the apparent exception of the Casimir effect). Since traversable wormholes in GR cannot be sourced by known matter sources, a natural question that arises is can wormholes without exotic matter be realized in modified theories of gravity.

Several modifications to Einstein's GR have been proposed to address its shortcomings. For example, observations of type-Ia supernovae and the cosmic microwave background have confirmed the accelerated expansion of the Universe. In the Λ -CDM model of cosmology based on GR, additional fields are required to describe the accelerated expansion of the Universe (the *dark energy* problem). However, in modified gravity theories, late-time cosmic accelerated expansion can be realized without any additional fields. Moreover, the gravitational field equations in modified gravity can be generalized to the following form [3]:

$$g_1(\psi^i)(G_{\mu\nu} + H_{\mu\nu}) - g_2(\psi^j)T_{\mu\nu} = \kappa T_{\mu\nu} \quad (3)$$

where $H_{\mu\nu}$ is an additional geometric term, $g_i(\psi^i)$ are multiplicative factors, and ψ^i are curvature invariants. Then, the matter threading wormhole geometries can satisfy the energy conditions provided

$$\frac{g_1(\psi^i)}{\kappa + g_1(\psi^j)}(G_{\mu\nu} + H_{\mu\nu})k^\mu k^\nu \geq 0 \quad (4)$$

Thus, owing to the inherently different structure of the field equations in modified gravity, wormhole solutions can be formulated with matter sources satisfying the energy conditions, and violations maybe attributed to additional curvature terms. To this end, traversable wormholes have been studied extensively in $f(R)$ modified gravity theory [4, 5, 6], which is perhaps the most extensively discussed modification of GR [7, 8]. Moreover, $f(R)$ theories are of significant interest in cosmology with regard to inflation and late-time acceleration of the observable Universe [9, 10, 11, 12, 13], and recently, in the context of gravitational waves [14, 15]. Recently, traversable wormhole solutions have been studied extensively in different $f(R)$ gravity theories with different choices of metric parameters [16, 17, 18, 19, 20, 21, 22, 23, 24]. Wormholes supported by ordinary matter in $f(R)$ gravity have also been reported previously [25, 26]. In this study, we focus on a recently proposed $f(R)$ gravity model [27, 28], and analyze the energy conditions for Morris-Thorne wormhole solutions. We explore four possible solutions with different choices of $\Phi(r)$ and $b(r)$, and demonstrate that traversable wormholes satisfying the energy conditions can be obtained in this theory with suitable choices of parameters.

The remainder of this manuscript is organized as follows: in Sec. 2, we describe the basic features of Morris-Thorne wormholes in $f(R)$ gravity, introduce the new model studied, and setup the field equations. In Sec. 3, we present our main results. We present relevant discussions in Sec. 4, and conclude the manuscript in Sec. 5. Throughout the manuscript, we adhere to natural units with $G = c = 1$.

2 The Morris-Thorne Wormhole in $f(R)$ gravity

In $f(R)$ gravity, the standard Einstein-Hilbert action takes the following form:

$$S = \int d^4x \sqrt{-g} [f(R) + \mathcal{L}_m] \quad (5)$$

where $f(R)$ is a function of the Ricci scalar, and \mathcal{L}_m collectively denotes the matter Lagrangian for possible matter fields. In the metric formalism, the following field equation gives the modified EFE for $f(R)$ gravity:

$$FR_{\mu\nu} - \frac{1}{2}f(R)g_{\mu\nu} - \nabla_\mu \nabla_\nu F + g_{\mu\nu} \square F = T_{\mu\nu}^m, \quad (6)$$

where $F \equiv df(R)/dR$, and $T_{\mu\nu}^m = \frac{-2}{\sqrt{-g}} \frac{\delta \mathcal{L}_m}{\delta g^{\mu\nu}}$ denotes the matter stress-energy tensor. We assume that $g_{\mu\nu}$ describes a spherically symmetric space-time described by the line-element in Eq. (1). The field equation Eq. (6) can be contracted to yield the following:

$$FR - 2f(R) + 3\square F = T \quad (7)$$

Here, T is the trace of the matter stress energy tensor and $\square F$ is given by the following expression, with $F' = df(R)/dR$ and $b' = db(r)/dr$:

$$\square F = \frac{1}{\sqrt{-g}} \partial_\mu (\sqrt{-g} g^{\mu\nu} \partial_\nu F) = \left(1 - \frac{b}{r}\right) \left[F'' - \frac{b'r - b}{2r^2(1 - b/r)} F' + \frac{2F'}{r} \right] \quad (8)$$

It can be verified that GR (without a cosmological constant) is recovered by setting $f(R) = R$ in Eq. (5), which implies $F = 1$, and $\square F = 0$. However, $\square F \neq 0$ in modified gravity theories, and it is generally interpreted as a propagating scalar degree of freedom. Now, substituting Eq. (4) in Eq. (6) yields the following modified EFE:

$$G_{\mu\nu} \equiv R_{\mu\nu} - \frac{1}{2}g_{\mu\nu}R = T_{\mu\nu}^{\text{eff}} \quad (9)$$

Here, $T_{\mu\nu}^{\text{eff}}$ is an effective stress-energy tensor, which may be interpreted as a gravitational fluid responsible for NEC violations in wormhole solutions. It contains the matter stress energy tensor $T_{\mu\nu}^m$ and curvature stress-energy tensor $T_{\mu\nu}^c$ given by:

$$T_{\mu\nu}^c = \frac{1}{F} \left[\nabla_\mu \nabla_\nu F - \frac{1}{4}g_{\mu\nu} (RF + \square F + T) \right] \quad (10)$$

We assume an anisotropic distribution of matter threading the wormhole geometry described by the following diagonal stress-energy tensor:

$$T_{\mu\nu} = (\rho + p_t)U_\mu U_\nu + p_t g_{\mu\nu} + (p_r - p_t)\chi_\mu \chi_\nu, \quad (11)$$

where U^μ is a four-velocity, and χ^μ is a unit space-like vector. The effective field equation Eq. (10) can be rearranged to yield the following expressions [4]:

$$\frac{b'}{r^2} = \frac{\rho}{F} + \frac{H}{F} \quad (12)$$

$$-\frac{b}{r^3} = \frac{p_r}{F} + \frac{1}{F} \left\{ \left(1 - \frac{b}{r}\right) \times \left[F'' - F' \frac{b'r - b}{2r^2(1 - b/r)} \right] - H \right\} \quad (13)$$

$$-\frac{b'r - b}{2r^3} = \frac{p_t}{F} + \frac{1}{F} \left[\left(1 - \frac{b}{r}\right) \frac{F'}{r} - H \right] \quad (14)$$

where $H(r) = \frac{1}{4}(FR + \square F + T)$ and $R = \frac{2b'}{r^2}$ in the background (1). Assuming $\Phi(r)' = 0$ for simplicity in the calculations, the field equations Eqs. (12)-(14) can be simplified to obtain the following:

$$\rho = \frac{Fb'}{r^2} \quad (15)$$

$$p_r = -\frac{bF}{r^3} + \frac{F'}{2r^2}(b'r - b) - F'' \left(1 - \frac{b}{r}\right) \quad (16)$$

$$p_t = -\frac{F'}{r} \left(1 - \frac{b}{r}\right) + \frac{F}{2r^3}(b - b'r) \quad (17)$$

However, the redshift function plays a crucial role in determining the behavior of the energy condition inequalities for wormholes. Thus, assuming a constant $\Phi(r)$ throughout the space-time might be an over simplification. We address this issue by studying wormhole solutions with a variable shape function. With $\Phi(r) \neq 0$, Eqs. (15)-(17) take the following form:

$$\rho = \frac{Fb'(r)}{r^2} - \left(1 - \frac{b(r)}{r}\right) F' \phi'(r) - H \quad (18)$$

$$p_r = -\frac{b(r)F}{r^3} + 2 \left(1 - \frac{b(r)}{r}\right) \frac{\phi'(r)F}{r} - \left(1 - \frac{b(r)}{r}\right) \left[F'' + \frac{F'(rb'(r) - b(r))}{2r^2 \left(1 - \frac{b(r)}{r}\right)} \right] + H \quad (19)$$

$$p_t = \frac{F(b(r) - rb'(r))}{2r^3} - \frac{F'}{r} \left(1 - \frac{b(r)}{r}\right) + F \left(1 - \frac{b(r)}{r}\right) \left(\phi''(r) - \frac{(rb'(r) - b(r))\phi'(r)}{2r(r - b)} + \phi'^2(r) + \frac{\phi'(r)}{r} \right) + H \quad (20)$$

Here, we consider a recently proposed viable $f(R)$ gravity model [27, 28] with:

$$f(R) = R - \frac{\alpha}{\pi} R_c \cot^{-1} \left(\frac{R_c^2}{R^2} \right) - \beta R_c \left[1 - \exp \left(-\frac{R}{R_c} \right) \right] \quad (21)$$

where α and β are dimensionless constants, and R_c is a characteristic curvature constant. This theory fulfills the basic requirements for a viable $f(R)$ theory [29, 13] for suitable choices of α , β , and R_c , including solar system tests. Moreover, the model has been investigated thoroughly in terms of observational constraints such as gravitational wave polarization modes and recent data from pulsar timing arrays [28], which may have important implications in certain astrophysical and cosmological problems. With this choice of $f(R)$, the energy condition inequalities can be examined via Eqs. (15)-(17) with suitable choices of $b(r)$ and $\Phi(r)$. In addition, we examine the equation of state (EoS) parameter, $\omega = p_r/\rho$, and anisotropy parameter, $\Delta = p_t - p_r$, for possible wormhole solutions. In our analyses, we consider the following two cases:

1. Case I: Constant redshift function

(a) constant $\Phi(r)$ with $b(r) = r_0 + r_0 \left[\left(\frac{r}{r_0} \right)^\gamma - 1 \right]$

(b) constant $\Phi(r)$ with $b(r) = \frac{r_0 \log(r+1)}{\log(r_0+1)}$

2. Case II: Variable redshift function

(a) $\Phi(r) = \sqrt{\frac{r_0}{r}}$ and $b(r) = r_0 \left[\left(\frac{r}{r_0} \right)^\gamma - 1 \right] + r_0$

(b) $\Phi(r) = \sqrt{\frac{r_0}{r}}$ and $b(r) = r_0 \log \left(\frac{r}{r_0} \right) + r_0$

2.1 Case I

2.1.1 Case I(a)

Here, we assume the redshift function to be constant for simplicity, and use the following functional form for the shape function [30]:

$$b(r) = r_0 \left[\left(\frac{r}{r_0} \right)^\gamma - 1 \right] + r_0 \quad (22)$$

where γ is a dimensionless constant in the range $0 < \gamma < 1$, imposed in order for Eq. (22) to satisfy the constraints on $b(r)$ described in Sec. 1. This shape function has been used previously to realize analytic wormhole solutions in GR, and it was demonstrated that the parameter γ has an important role in determining energy condition violations [30]. Asymptotically flat wormhole solutions were formulated analytically for specific choices of parameters, and here, we investigate the energy conditions numerically for the allowed range of γ from the aspect of energy condition violation. With this choice of $b(r)$, Eqs. (15)-(17) take the following form:

$$\rho = \frac{\gamma r_0 \left(\frac{r}{r_0} \right)^\gamma}{r^3} \left[-\frac{4\alpha\gamma R_c^3 r_0 r^9 \left(\frac{r}{r_0} \right)^\gamma}{\pi R_c^4 r^{12} + 16\pi\gamma^4 r_0^4 \left(\frac{r}{r_0} \right)^{4\gamma}} - \beta e^{-\frac{2\gamma r_0 \left(\frac{r}{r_0} \right)^\gamma}{R_c r^3}} + 1 \right] \quad (23)$$

$$\begin{aligned} p_r = & \frac{r_0 \left(\frac{r}{r_0} \right)^\gamma \left[\frac{4\alpha\gamma R_c^3 r_0 r^9 \left(\frac{r}{r_0} \right)^\gamma}{\pi R_c^4 r^{12} + 16\pi\gamma^4 r_0^4 \left(\frac{r}{r_0} \right)^{4\gamma}} + \beta e^{-\frac{2\gamma r_0 \left(\frac{r}{r_0} \right)^\gamma}{R_c r^3}} - 1 \right]}{r^3} \\ & + \frac{(\gamma - 1)r_0 \left(\frac{r}{r_0} \right)^\gamma \left[\frac{\beta e^{-\frac{2\gamma r_0 \left(\frac{r}{r_0} \right)^\gamma}{R_c r^3}}}{R_c} - \frac{2\alpha R_c^3 \left(R_c^4 - \frac{48\gamma^4 \left(\frac{r}{r_0} \right)^{4(\gamma-1)}}{r^8} \right)}{\pi \left(R_c^4 + \frac{16\gamma^4 \left(\frac{r}{r_0} \right)^{4(\gamma-1)}}{r^8} \right)^2} \right]}{2r^2} \\ & + \left[\left(\frac{r}{r_0} \right)^{\gamma-1} - 1 \right] \left[\frac{64\alpha\gamma^3 R_c^3 \left(\frac{r}{r_0} \right)^{3(\gamma-1)} \left(\frac{48\gamma^4 \left(\frac{r}{r_0} \right)^{4(\gamma-1)}}{r^8} - 5R_c^4 \right)}{\pi r^6 \left(R_c^4 + \frac{16\gamma^4 \left(\frac{r}{r_0} \right)^{4(\gamma-1)}}{r^8} \right)^3} - \frac{\beta e^{-\frac{2\gamma r_0 \left(\frac{r}{r_0} \right)^\gamma}{R_c r^3}}}{R_c^2} \right] \end{aligned} \quad (24)$$

$$\begin{aligned}
p_t = & -\frac{(\gamma-1)r_0\left(\frac{r}{r_0}\right)^\gamma\left[-\frac{4\alpha\gamma R_c^3 r_0^9\left(\frac{r}{r_0}\right)^\gamma}{\pi R_c^4 r^{12}+16\pi\gamma^4 r_0^4\left(\frac{r}{r_0}\right)^{4\gamma}}-\beta e^{-\frac{2\gamma r_0\left(\frac{r}{r_0}\right)^\gamma}{R_c r^3}}+1\right]}{2r^3}+\left[\left(\frac{r}{r_0}\right)^{\gamma-1}-1\right] \\
& \times \frac{\left[\frac{\beta e^{-\frac{2\gamma r_0\left(\frac{r}{r_0}\right)^\gamma}{R_c r^3}}}{R_c}-\frac{2\alpha R_c^3\left(R_c^4-\frac{48\gamma^4\left(\frac{r}{r_0}\right)^{4(\gamma-1)}}{r^8}\right)}{\pi\left(R_c^4+\frac{16\gamma^4\left(\frac{r}{r_0}\right)^{4(\gamma-1)}}{r^8}\right)^2}\right]}{r}
\end{aligned} \tag{25}$$

2.1.2 Case I(b)

Here, we adopt the following logarithmic shape function satisfying the necessary conditions for a Morris-Thorne wormhole [16]:

$$b(r) = \frac{r_o \log(r+1)}{\log(r_o+1)} \tag{26}$$

Substituting Eq. (26) into Eqs. (15)-(17), we obtain the following:

$$\rho = \frac{r_o \left[1 - \beta e^{\frac{-2r_o}{R_c r^2(1+r) \log(r_o+1)}}\right] - \frac{4R_c^3 r_o r^6 (1+r_o)^3 \alpha \log(1+r_o)^3}{16\pi r_o^4 + R_c^4 \pi r^8 (1+r)^4 \log(1+r_o)^4}}{r^2 (1+r) \log(1+r_o)} \tag{27}$$

$$\begin{aligned}
p_r = & -\frac{r_o \left[1 - \beta e^{\frac{-2r_o}{R_c r^2(1+r) \log(1+r_o)}} - \frac{4R_c^3 r_o r^6 \alpha \log(1+r_o)^3 (1+r)^3}{16\pi r_o^4 + R_c^4 \pi r^8 (1+r)^4 \log(1+r_o)^4}\right]}{r^3 \log(1+r_o)} \log(1+r) \\
& - \frac{r_o \left[\frac{\beta e^{\frac{-2r_o}{R_c r^2(1+r) \log(1+r_o)}}}{R_c} - \frac{2R_c^3 \alpha \left(R_c^4 - \frac{48r_o^4}{r^8(1+r)^4}\right)}{\pi \left(R_c^4 + \frac{16r_o^4}{r^8(1+r)^4 \log(1+r_o)^4}\right)^2}\right]}{2r^2 (1+r) \log(1+r_o)} [-r + (1+r) \log(1+r)] \\
& - \left[-\frac{\beta e^{\frac{-2r_o}{R_c r^2(1+r) \log(1+r_o)}}}{R_c^2} + \frac{64R_c^3 r_o^3 r^{10} (1+r)^5 \alpha \log(1+r_o)^5 \left(48r_o^4 - 5R_c^4 r^8 (1+r)^4 \log(1+r_o)^4\right)}{\pi \left(16r_o^4 + R_c^4 r^8 (1+r)^4 \log(1+r_o)^4\right)^3}\right] \\
& \times \left[1 - \frac{r_o \log(1+r)}{r \log(1+r_o)}\right]
\end{aligned} \tag{28}$$

$$\begin{aligned}
p_t = & \frac{r_o \left[1 - \beta e^{\frac{-2r_o}{R_c r^4(1+r) \log(1+r_c)}} - \frac{4R_c^3 r_o r^6 (1+r)^3 \alpha \log(1+r_o)^3}{16\pi r_o^4 + R_c^4 \pi r^8 (1+r)^4 \log(1+r_o)^4}\right]}{2r^3 (1+r) \log(1+r_o)} \left[-r + (1+r) \log(1+r)\right] - \left[1 - \frac{r_o \log(1+r)}{r \log(1+r_o)}\right] \\
& \times \frac{\left[\frac{\beta e^{\frac{-2r_o}{R_c r^2(1+r) \log(1+r_o)}}}{R_c} - \frac{2R_c^3 \alpha \left(\frac{48r_o^4}{r^8(1+r)^4 \log(1+r_o)^4}\right)}{\pi \left(R_c^4 + \frac{16r_o^4}{r^8(1+r)^4 \log(1+r_o)^4}\right)^2}\right]}{r^2}
\end{aligned} \tag{29}$$

2.2 Case II

2.2.1 Case II(a)

Here, we adopt the following combination of $\Phi(r)$ and $b(r)$

$$\Phi(r) = \sqrt{\frac{r_0}{r}} \tag{30}$$

$$b(r) = r_0 \left[\left(\frac{r}{r_0}\right)^\gamma - 1\right] + r_0 \tag{31}$$

In this case, Eqs. (18)-(20) take the following forms:

$$\begin{aligned}
\rho = & \frac{1}{2} \left[-\frac{\alpha R_c \cot^{-1} \left(\frac{R_c^2 r^4 \left(\frac{r}{r_0} \right)^{2-2\gamma}}{4\gamma^2} \right)}{\pi} + \beta R_c \left(e^{-\frac{2\gamma r_0 \left(\frac{r}{r_0} \right)^\gamma}{R_c r^3}} - 1 \right) + \frac{2\gamma r_0 \left(\frac{r}{r_0} \right)^\gamma}{r^3} \right] \\
& + \frac{\sqrt{\frac{r_0}{r}} \left(1 - \left(\frac{r}{r_0} \right)^{\gamma-1} \right) \left(-\frac{4\alpha\gamma R_c^3 r_0 r^9 \left(\frac{r}{r_0} \right)^\gamma}{\pi R_c^4 r^{12} + 16\pi\gamma^4 r_0^4 \left(\frac{r}{r_0} \right)^{4\gamma}} - \beta e^{-\frac{2\gamma r_0 \left(\frac{r}{r_0} \right)^\gamma}{R_c r^3}} + 1 \right)}{2r} - \left[1 - \left(\frac{r}{r_0} \right)^{\gamma-1} \right] \\
& \times \left[-\frac{8\alpha R_c^7 r^{24}}{\pi \left(R_c^4 r^{12} + 16\gamma^4 r_0^4 \left(\frac{r}{r_0} \right)^{4\gamma} \right)^2} + \frac{6\alpha R_c^3 r^{12}}{\pi R_c^4 r^{12} + 16\pi\gamma^4 r_0^4 \left(\frac{r}{r_0} \right)^{4\gamma}} \right. \\
& + \frac{2\alpha\gamma R_c^3 r_0 r^8 \left(r_0 \left(\frac{r}{r_0} \right)^\gamma (\gamma + \sqrt{\frac{r_0}{r}} - 5) - r (\sqrt{\frac{r_0}{r}} - 4) \right) \left(\frac{r}{r_0} \right)^\gamma}{\pi \left(r_0 \left(\frac{r}{r_0} \right)^\gamma - r \right) \left(R_c^4 r^{12} + 16\gamma^4 r_0^4 \left(\frac{r}{r_0} \right)^{4\gamma} \right)} + \frac{\beta e^{-\frac{2\gamma r_0 \left(\frac{r}{r_0} \right)^\gamma}{R_c r^3}}}{R_c} \\
& \left. + \frac{\left(r_0 \left(\frac{r}{r_0} \right)^\gamma (\gamma + \sqrt{\frac{r_0}{r}} - 5) - r (\sqrt{\frac{r_0}{r}} - 4) \right) e^{-\frac{2\gamma r_0 \left(\frac{r}{r_0} \right)^\gamma}{R_c r^3}} \left(e^{\frac{2\gamma r_0 \left(\frac{r}{r_0} \right)^\gamma}{R_c r^3}} - \beta \right)}{2r \left(r - r_0 \left(\frac{r}{r_0} \right)^\gamma \right)} \right] \quad (32)
\end{aligned}$$

$$\begin{aligned}
p_r = & \frac{1}{2} \left[\frac{\alpha R_c \left(-4r^2 \sqrt{\frac{r_0}{r}} - 2(\gamma - 1)r_0 \left(\frac{r}{r_0} \right)^\gamma + 4r_0 r \sqrt{\frac{r_0}{r}} \left(\frac{r}{r_0} \right)^\gamma + r^3 \right) \cot^{-1} \left(\frac{R_c^2 r^4 \left(\frac{r}{r_0} \right)^{2-2\gamma}}{4\gamma^2} \right)}{\pi r^3} \right. \\
& + \frac{4\alpha\gamma R_c^3 r_0 r^8 \left(\sqrt{\frac{r_0}{r}} - 4 \right) \left(\frac{r}{r_0} \right)^\gamma}{\pi \left(R_c^4 r^{12} + 16\gamma^4 r_0^4 \left(\frac{r}{r_0} \right)^{4\gamma} \right)} - \frac{4\alpha\gamma R_c^3 r_0^2 r^7 \left(\sqrt{\frac{r_0}{r}} - 4 \right) \left(\frac{r}{r_0} \right)^{2\gamma}}{\pi \left(R_c^4 r^{12} + 16\gamma^4 r_0^4 \left(\frac{r}{r_0} \right)^{4\gamma} \right)} + \beta R_c \left\{ 1 - e^{-\frac{2\gamma r_0 \left(\frac{r}{r_0} \right)^\gamma}{R_c r^3}} \right\} \\
& + \frac{\beta \left(4R_c \sqrt{\frac{r_0}{r}} + \sqrt{\frac{r_0}{r}} - 4 \right) e^{-\frac{2\gamma r_0 \left(\frac{r}{r_0} \right)^\gamma}{R_c r^3}} - 4\beta R_c \sqrt{\frac{r_0}{r}} - \sqrt{\frac{r_0}{r}} + 4}{r} \\
& + \frac{2r_0 \left(\frac{r}{r_0} \right)^\gamma \left(\beta(\gamma - 1)R_c \left(-e^{-\frac{2\gamma r_0 \left(\frac{r}{r_0} \right)^\gamma}{R_c r^3}} \right) \left(e^{\frac{2\gamma r_0 \left(\frac{r}{r_0} \right)^\gamma}{R_c r^3}} - 1 \right) - \gamma \right)}{r^3} \\
& + \frac{r_0 \left(\frac{r}{r_0} \right)^\gamma \left(-\beta \left(4R_c \sqrt{\frac{r_0}{r}} + \sqrt{\frac{r_0}{r}} - 4 \right) e^{-\frac{2\gamma r_0 \left(\frac{r}{r_0} \right)^\gamma}{R_c r^3}} + 4\beta R_c \sqrt{\frac{r_0}{r}} + \sqrt{\frac{r_0}{r}} - 4 \right)}{r^2} + \frac{4(\gamma - 1)\gamma r_0^2 \left(\frac{r}{r_0} \right)^{2\gamma}}{r^6} \\
& \left. + \frac{8\gamma \left(\frac{r_0}{r} \right)^{3/2} \left(\frac{r}{r_0} \right)^\gamma}{r^3} - \frac{8\gamma \left(\frac{r_0}{r} \right)^{5/2} \left(\frac{r}{r_0} \right)^{2\gamma}}{r^3} \right] \quad (33)
\end{aligned}$$

$$\begin{aligned}
p_t = & \frac{1}{2} \left[\frac{2 \left(\frac{2r_0\gamma \left(\frac{r}{r_0}\right)^\gamma}{r^3} + \left(-1 + e^{-\frac{2r_0\left(\frac{r}{r_0}\right)^\gamma \gamma}{R_c r^3}} \right) R_c \beta - \frac{R_c \alpha \cot^{-1} \left(\frac{R_c^2 r^4 \left(\frac{r}{r_0}\right)^{2-2\gamma}}{4\gamma^2} \right)}{\pi} \right) r_0 \gamma \left(\frac{r}{r_0}\right)^\gamma}{r^3} \right. \\
& - \frac{r_0(\gamma-1) \left(\frac{2r_0\gamma \left(\frac{r}{r_0}\right)^\gamma}{r^3} + \left(-1 + e^{-\frac{2r_0\left(\frac{r}{r_0}\right)^\gamma \gamma}{R_c r^3}} \right) R_c \beta - \frac{R_c \alpha \cot^{-1} \left(\frac{R_c^2 r^4 \left(\frac{r}{r_0}\right)^{2-2\gamma}}{4\gamma^2} \right)}{\pi} \right) \left(\frac{r}{r_0}\right)^\gamma}{r^2} - \frac{2r_0\gamma \left(\frac{r}{r_0}\right)^\gamma}{r^3} \\
& + \left\{ 1 - e^{-\frac{2r_0\left(\frac{r}{r_0}\right)^\gamma \gamma}{R_c r^3}} \right\} R_c \beta + 2 \left\{ 1 - \left(\frac{r}{r_0}\right)^{\gamma-1} \right\} \\
& \times \left\{ \frac{2R_c^3 r_0 r^8 \alpha \gamma \left(r_0 \left(\frac{r}{r_0}\right)^\gamma (\gamma + \sqrt{\frac{r_0}{r}} - 5) - (\sqrt{\frac{r_0}{r}} - 4) r \right) \left(\frac{r}{r_0}\right)^\gamma}{\pi \left(r_0 \left(\frac{r}{r_0}\right)^\gamma - r \right) \left(16r_0^4 \gamma^4 \left(\frac{r}{r_0}\right)^{4\gamma} + R_c^4 r^{12} \right)} + \frac{e^{-\frac{2r_0\left(\frac{r}{r_0}\right)^\gamma \gamma}{R_c r^3}} \beta}{R_c} \right. \\
& + \frac{e^{-\frac{2r_0\left(\frac{r}{r_0}\right)^\gamma \gamma}{R_c r^3}} \left(e^{\frac{2r_0\left(\frac{r}{r_0}\right)^\gamma \gamma}{R_c r^3}} - \beta \right) \left(r_0 \left(\frac{r}{r_0}\right)^\gamma (\gamma + \sqrt{\frac{r_0}{r}} - 5) - (\sqrt{\frac{r_0}{r}} - 4) r \right)}{2r \left(r - r_0 \left(\frac{r}{r_0}\right)^\gamma \right)} - \frac{8R_c^7 r^{24} \alpha}{\pi \left(16r_0^4 \gamma^4 \left(\frac{r}{r_0}\right)^{4\gamma} + R_c^4 r^{12} \right)^2} \\
& + \left. \frac{6R_c^3 r^{12} \alpha}{16\pi r_0^4 \gamma^4 \left(\frac{r}{r_0}\right)^{4\gamma} + R_c^4 \pi r^{12}} \right\} + \frac{R_c \alpha \cot^{-1} \left(\frac{R_c^2 r^4 \left(\frac{r}{r_0}\right)^{2-2\gamma}}{4\gamma^2} \right)}{\pi} + \frac{e^{-\frac{2r_0\left(\frac{r}{r_0}\right)^\gamma \gamma}{R_c r^3}} \left(r_0(\gamma-2) \left(\frac{r}{r_0}\right)^\gamma + r \right)}{2\pi r^6} \\
& \times \left\{ \left(2e^{\frac{2r_0\left(\frac{r}{r_0}\right)^\gamma \gamma}{R_c r^3}} \pi r_0 \gamma \left(\frac{r}{r_0}\right)^\gamma - \left(-1 + e^{\frac{2r_0\left(\frac{r}{r_0}\right)^\gamma \gamma}{R_c r^3}} \right) R_c \pi r^3 \beta \right. \right. \\
& - \left. \left. e^{\frac{2r_0\left(\frac{r}{r_0}\right)^\gamma \gamma}{R_c r^3}} R_c r^3 \alpha \cot^{-1} \left(\frac{R_c^2 r^4 \left(\frac{r}{r_0}\right)^{2-2\gamma}}{4\gamma^2} \right) \right) \sqrt{\frac{r_0}{r}} \right\} \\
& - \left. \frac{2 \left(1 - \left(\frac{r}{r_0}\right)^{\gamma-1} \right) \left(-\frac{4R_c^3 r_0 r^9 \alpha \gamma \left(\frac{r}{r_0}\right)^\gamma}{16\pi r_0^4 \gamma^4 \left(\frac{r}{r_0}\right)^{4\gamma} + R_c^4 \pi r^{12}} - e^{-\frac{2r_0\left(\frac{r}{r_0}\right)^\gamma \gamma}{R_c r^3}} \beta + 1 \right)}{r} \right] \quad (34)
\end{aligned}$$

2.2.2 Case II(b)

Here, we adopt the following combination of $\Phi(r)$ and $b(r)$

$$\Phi(r) = \sqrt{\frac{r_0}{r}} \quad (35)$$

$$b(r) = r_0 \log \left(\frac{r}{r_0} \right) + r_0 \quad (36)$$

In this case, Eqs. (18)-(20) take the following forms:

$$\begin{aligned}
\rho = & \frac{1}{2} \left[-\frac{\alpha R_c \cot^{-1} \left(\frac{R_c^2 r^6}{4r_0^2} \right)}{\pi} + \frac{\sqrt{\frac{r_0}{r}} \left(1 - \frac{r_0 \left(\log \left(\frac{r}{r_0} \right) + 1 \right)}{r} \right) \left(-\frac{4\alpha R_c^3 r_0 r^9}{\pi R_c^4 r^{12} + 16\pi r_0^4} - \beta e^{-\frac{2r_0}{R_c r^3}} + 1 \right)}{r} \right. \\
& - 2 \left\{ 1 - \frac{r_0 \left(\log \left(\frac{r}{r_0} \right) + 1 \right)}{r} \right\} \left\{ -\frac{8\alpha R_c^7 r^{24}}{\pi (R_c^4 r^{12} + 16r_0^4)^2} + \frac{6\alpha R_c^3 r^{12}}{\pi R_c^4 r^{12} + 16\pi r_0^4} + \frac{2\alpha R_c^3 r_0 r^8 \left(\sqrt{\frac{r_0}{r}} - 4 \right)}{\pi (R_c^4 r^{12} + 16r_0^4)} \right. \\
& + \frac{r_0 \log \left(\frac{r}{r_0} \right) \left(-\frac{4\alpha R_c^3 r_0 r^9}{\pi R_c^4 r^{12} + 16\pi r_0^4} - \beta e^{-\frac{2r_0}{R_c r^3}} + 1 \right)}{2r \left(r_0 \log \left(\frac{r}{r_0} \right) + r_0 - r \right)} + \frac{\beta e^{-\frac{2r_0}{R_c r^3}}}{R_c} - \frac{(\sqrt{\frac{r_0}{r}} - 4) e^{-\frac{2r_0}{R_c r^3}} \left(e^{\frac{2r_0}{R_c r^3}} - \beta \right)}{2r} \left. \right\} \\
& + \beta R_c \left(e^{-\frac{2r_0}{R_c r^3}} - 1 \right) + \frac{2r_0}{r^3} \left. \right] \tag{37}
\end{aligned}$$

$$\begin{aligned}
p_r = & \frac{1}{2} \left[\frac{\alpha R_c \cot^{-1} \left(\frac{R_c^2 r^6}{4r_0^2} \right)}{\pi} - \frac{4\alpha R_c \sqrt{\frac{r_0}{r}} \cot^{-1} \left(\frac{R_c^2 r^6}{4r_0^2} \right)}{\pi r} + \frac{4\alpha R_c \left(\frac{r_0}{r} \right)^{3/2} \left(\log \left(\frac{r}{r_0} \right) + 1 \right) \cot^{-1} \left(\frac{R_c^2 r^6}{4r_0^2} \right)}{\pi r} \right. \\
& + \frac{2\alpha R_c r_0 \log \left(\frac{r}{r_0} \right) \cot^{-1} \left(\frac{R_c^2 r^6}{4r_0^2} \right)}{\pi r^3} + \frac{4 \left(-\frac{4\alpha R_c^3 r_0 r^9}{\pi R_c^4 r^{12} + 16\pi r_0^4} - \beta e^{-\frac{2r_0}{R_c r^3}} + 1 \right)}{r} \\
& - \frac{\sqrt{\frac{r_0}{r}} \left(-\frac{4\alpha R_c^3 r_0 r^9}{\pi R_c^4 r^{12} + 16\pi r_0^4} - \beta e^{-\frac{2r_0}{R_c r^3}} + 1 \right)}{r} + \frac{\left(\frac{r_0}{r} \right)^{3/2} \left(\log \left(\frac{r}{r_0} \right) + 1 \right) \left(-\frac{4\alpha R_c^3 r_0 r^9}{\pi R_c^4 r^{12} + 16\pi r_0^4} - \beta e^{-\frac{2r_0}{R_c r^3}} + 1 \right)}{r} \\
& - \frac{4r_0 \left(\log \left(\frac{r}{r_0} \right) + 1 \right) \left(-\frac{4\alpha R_c^3 r_0 r^9}{\pi R_c^4 r^{12} + 16\pi r_0^4} - \beta e^{-\frac{2r_0}{R_c r^3}} + 1 \right)}{r^2} + \beta R_c \left(1 - e^{-\frac{2r_0}{R_c r^3}} \right) - \frac{4\beta R_c \sqrt{\frac{r_0}{r}} \left(1 - e^{-\frac{2r_0}{R_c r^3}} \right)}{r} \\
& + \frac{4\beta R_c \left(\frac{r_0}{r} \right)^{3/2} \left(1 - e^{-\frac{2r_0}{R_c r^3}} \right) \left(\log \left(\frac{r}{r_0} \right) + 1 \right)}{r} + \frac{2\beta R_c r_0 \left(1 - e^{-\frac{2r_0}{R_c r^3}} \right) \log \left(\frac{r}{r_0} \right)}{r^3} - \frac{4r_0^2 \log \left(\frac{r}{r_0} \right)}{r^6} \\
& + \frac{8 \left(\frac{r_0}{r} \right)^{3/2}}{r^3} - \frac{2r_0}{r^3} - \frac{8 \left(\frac{r_0}{r} \right)^{5/2} \left(\log \left(\frac{r}{r_0} \right) + 1 \right)}{r^3} \left. \right] \tag{38}
\end{aligned}$$

$$\begin{aligned}
p_t = & \frac{1}{2} \left[\frac{\alpha R_c \cot^{-1} \left(\frac{R_c^2 r^6}{4r_0^2} \right)}{\pi} + \frac{2r_0 \left(-\frac{\alpha R_c \cot^{-1} \left(\frac{R_c^2 r^6}{4r_0^2} \right)}{\pi} + \beta R_c \left(e^{-\frac{2r_0}{R_c r^3}} - 1 \right) + \frac{2r_0}{r^3} \right)}{r^3} \right. \\
& - \frac{\sqrt{\frac{r_0}{r}} e^{-\frac{2r_0}{R_c r^3}} \left(2r_0 \log \left(\frac{r}{r_0} \right) + r_0 - r \right) \left(-\alpha R_c r^3 e^{\frac{2r_0}{R_c r^3}} \cot^{-1} \left(\frac{R_c^2 r^6}{4r_0^2} \right) + \pi e^{\frac{2r_0}{R_c r^3}} (2r_0 - \beta R_c r^3) + \pi \beta R_c r^3 \right)}{2\pi r^6} \\
& + \frac{r_0 \log \left(\frac{r}{r_0} \right) \left(-\frac{\alpha R_c \cot^{-1} \left(\frac{R_c^2 r^6}{4r_0^2} \right)}{\pi} + \beta R_c \left(e^{-\frac{2r_0}{R_c r^3}} - 1 \right) + \frac{2r_0}{r^3} \right)}{r^2} \\
& - \frac{2 \left(1 - \frac{r_0 \left(\log \left(\frac{r}{r_0} \right) + 1 \right)}{r} \right) \left(-\frac{4\alpha R_c^3 r_0 r^9}{\pi R_c^4 r^{12} + 16\pi r_0^4} - \beta e^{-\frac{2r_0}{R_c r^3}} + 1 \right)}{r} + 2 \left\{ 1 - \frac{r_0 \left(\log \left(\frac{r}{r_0} \right) + 1 \right)}{r} \right\} \left. \right]
\end{aligned}$$

$$\begin{aligned}
& \times \left\{ -\frac{8\alpha R_c^7 r^{24}}{\pi (R_c^4 r^{12} + 16r_0^4)^2} + \frac{6\alpha R_c^3 r^{12}}{\pi R_c^4 r^{12} + 16\pi r_0^4} + \frac{2\alpha R_c^3 r_0 r^8 (\sqrt{\frac{r_0}{r}} - 4)}{\pi (R_c^4 r^{12} + 16r_0^4)} + \frac{\beta e^{-\frac{2r_0}{R_c r^3}}}{R_c} \right. \\
& + \frac{r_0 \log\left(\frac{r}{r_0}\right) \left(-\frac{4\alpha R_c^3 r_0 r^9}{\pi R_c^4 r^{12} + 16\pi r_0^4} - \beta e^{-\frac{2r_0}{R_c r^3}} + 1 \right)}{2r \left(r_0 \log\left(\frac{r}{r_0}\right) + r_0 - r \right)} - \frac{(\sqrt{\frac{r_0}{r}} - 4) e^{-\frac{2r_0}{R_c r^3}} \left(e^{\frac{2r_0}{R_c r^3}} - \beta \right)}{2r} \Bigg\} \\
& + \left[\beta R_c \left(1 - e^{-\frac{2r_0}{R_c r^3}} \right) - \frac{2r_0}{r^3} \right]
\end{aligned} \tag{39}$$

3 Results

3.1 Constant redshift function

Case I(a): $b(r) = r_0 + r_0 \left[\left(\frac{r}{r_0} \right)^\gamma - 1 \right]$

Figs. 1(a-d) show plots of ρ , $\rho + p_r$, $\rho + p_t$, and $\rho + p_r + 2p_t$, respectively, for different combinations of model parameters in arbitrary units, with $R_c = 1$ and $r_0 = 0.9$. The results show that the energy density is positive for all values of $r > 0$, as shown in Fig. 1(a). This implies that the WEC is satisfied by the solution. Moreover, Fig. 1(b) shows that the first NEC inequality, $\rho + p_r \geq 0$ is not satisfied at the throat. However, the second NEC inequality, $\rho + p_t \geq 0$ holds at the throat (Fig. 2(c)). The SEC is violated at the throat for all γ , as shown in Fig. 1(d). Moreover, the EoS parameter ω is < -1 at the throat, and Δ is positive, implying a phantom-like matter source, and repulsive nature of the geometry at the throat, respectively.

Case I(b): $b(r) = \frac{r_0 \log(r+1)}{\log(r_0+1)}$

Figs. 2(a-d) show plots of ρ , $\rho + p_r$, $\rho + p_t$, and $\rho + p_r + 2p_t$, respectively, for different combinations of model parameters in arbitrary units, with $R_c = 1$ and $r_0 = 0.9$. The results have also been summarized in detail in Table 1. The results show that the energy density is positive for all values of $r > 0$, as shown in Fig. 2(a). This implies that the WEC is satisfied by our solution. Fig. 2(b) shows that the first NEC inequality, $\rho + p_r \geq 0$ is not satisfied at the throat. It can be seen that the inequality holds for regions far outside the throat, and thus, exotic matter can be considered to be confined to a small region near the throat. However, the second NEC inequality, $\rho + p_t \geq 0$ holds at the throat (Fig. 2(c)), and is violated away from it for higher values of model parameters (red and blue lines). Next, the SEC is violated for our solution at the throat, as seen in Fig. 2(d). In all cases, lower values of model parameters α and β restrict the exotic matter to arbitrarily small regions around the throat (with a slight deviation in $\rho + p_r$). Moreover, the EoS parameter ω is < -1 at the throat. These results show that traversable wormholes with a phantom-like source with NEC violations restricted to arbitrarily small regions near the throat can be realized in the model.

3.2 Variable redshift function

Case II(a): $\Phi(r) = \sqrt{\frac{r_0}{r}}$ and $b(r) = r_0 \left[\left(\frac{r}{r_0} \right)^\gamma - 1 \right] + r_0$

Figs. 3(a-d) show plots of ρ , $\rho + p_r$, $\rho + p_t$, and $\rho + p_r + 2p_t$, respectively, for different combinations of model parameters in arbitrary units, with $R_c = 1$ and $r_0 = 0.9$. In addition, we set $\alpha = 0.005$ and $\beta = 0.008$ in the following analyses, which is discussed further in Sec. 4. The results show that the energy density is positive at the throat, and violated away from it. Moreover, Figs. 1(b) and (c) show that the first NEC inequality, $\rho + p_r \geq 0$ is not satisfied at the throat, and the second NEC inequality, $\rho + p_t \geq 0$, holds at the throat. Next, the SEC is satisfied for $\gamma > 0.6$, as seen in Fig. 1(d). Moreover, the EoS parameter ω is < -1 at the throat, and Δ is positive. Thus, traversable wormholes with a phantom-like source can be realized in the model.

Table 1: Summary of results for Case I(b).

Term	Result	Interpretation
ρ	$> 0 \forall r$ in all Cases	WEC satisfied
$\rho + p_r$	< 0 for $r \in (0, 1.8)$, > 0 for $r \in (1.8, \infty)$ with $\alpha = 0.15, \beta = 0.50$ < 0 for $r \in (0, 3.3)$, > 0 for $r \in (3.3, \infty)$ $\alpha = 0.05, \beta = 0.08$ < 0 for $r \in (0, 7.3)$, > 0 for $r \in (7.3, \infty)$ with $\alpha = 0.005, \beta = 0.008$	Not satisfied at the throat.
$\rho + p_t$	> 0 for $r \in (0, 2.7)$, < 0 for $r \in (2.7, \infty)$ with $\alpha = 0.15, \beta = 0.50$ > 0 for $r \in (0, 8.3)$, < 0 for $r \in (8.3, \infty)$ with $\alpha = 0.05, \beta = 0.08$ $\geq 0 \forall r$ with $\alpha = 0.005, \beta = 0.008$	Satisfied at throat
$\rho + p_r + 2p_t$	< 0 for $r \in (0.7, 1.9)$ and ≥ 0 otherwise with $\alpha = 0.15, \beta = 0.50$ < 0 for $r \in (0.7, 1.4)$ and ≥ 0 otherwise for $\alpha = 0.05, \beta = 0.08$ < 0 for $r \in (0.9, 1.4)$ and ≥ 0 otherwise for $\alpha = 0.005, \beta = 0.008$	Not satisfied in a small region around the throat
ω	< -1 near throat for all Cases	Phantom-matter source
Δ	> 0 near the throat	Repulsive geometry near throat

Table 2: Summary of results for Case II(b).

Term	Result	Interpretation
ρ	> 0 for $r \in (0, 1.9)$ and < 0 otherwise for $\alpha = 0.15, \beta = 0.50$ > 0 for $r \in (0, 2.3)$ < 0 otherwise for $\alpha = 0.05, 0.005$ and $\beta = 0.08, 0.008$	WEC satisfied at throat
$\rho + p_r$	> 0 for $r \in (0, 0.9) \cup (1.2, 2.1)$; < 0 otherwise for $\alpha = 0.15, \beta = 0.50$ > 0 for $r \in (0, 0.9) \cup (1.2, 7.2)$; < 0 otherwise for $\alpha = 0.05, \beta = 0.08$ < 0 for $r \in (0.9, 1.2)$; ≥ 0 otherwise for $\alpha = 0.005, \beta = 0.008$	Satisfied at the throat
$\rho + p_t$	> 0 for $r \in (0, 1.9)$ and < 0 otherwise	Satisfied at throat
$\rho + p_r + 2p_t$	< 0 for $r \in (1.2, 1.8)$ and > 0 otherwise with $\alpha = 0.15, \beta = 0.50$ < 0 for $r \in (1.2, 2.3)$ and > 0 otherwise for $\alpha = 0.05, 0.005$ and $\beta = 0.08, 0.008$	SEC satisfied at throat
ω	< -1 at the throat	Phantom-matter source
Δ	> 0 at the throat	Repulsive geometry near throat

Case II(b): $b(r) = r_0 \log\left(\frac{r}{r_0}\right) + r_0$ and $\Phi(r) = \sqrt{\frac{r_0}{r}}$

Figs. 4(a-d) show plots of ρ , $\rho + p_r$, $\rho + p_t$, and $\rho + p_r + 2p_t$, respectively, for different combinations of model parameters in arbitrary units, with $R_c = 1$ and $r_0 = 0.9$. The results have also been presented in detail in Table 2. The results show that the energy density is positive at the throat, as shown in Fig. 1(a). Moreover, Figs. 1(b) and (c) show that the NEC inequalities $\rho + p_r \geq 0$ and $\rho + p_t \geq 0$ hold at the throat. In addition, the SEC is satisfied at the throat and away from it, with violations in a small region near the throat, as shown in Fig. 1(d). Here, lower values of the parameters α and β restrict SEC violation to a small region around the throat. The EoS parameter is < -1 near the throat, and Δ is positive near the throat. Thus, a traversable wormhole solution satisfying the energy conditions at the throat can be realized in this case, sourced by a phantom-like fluid.

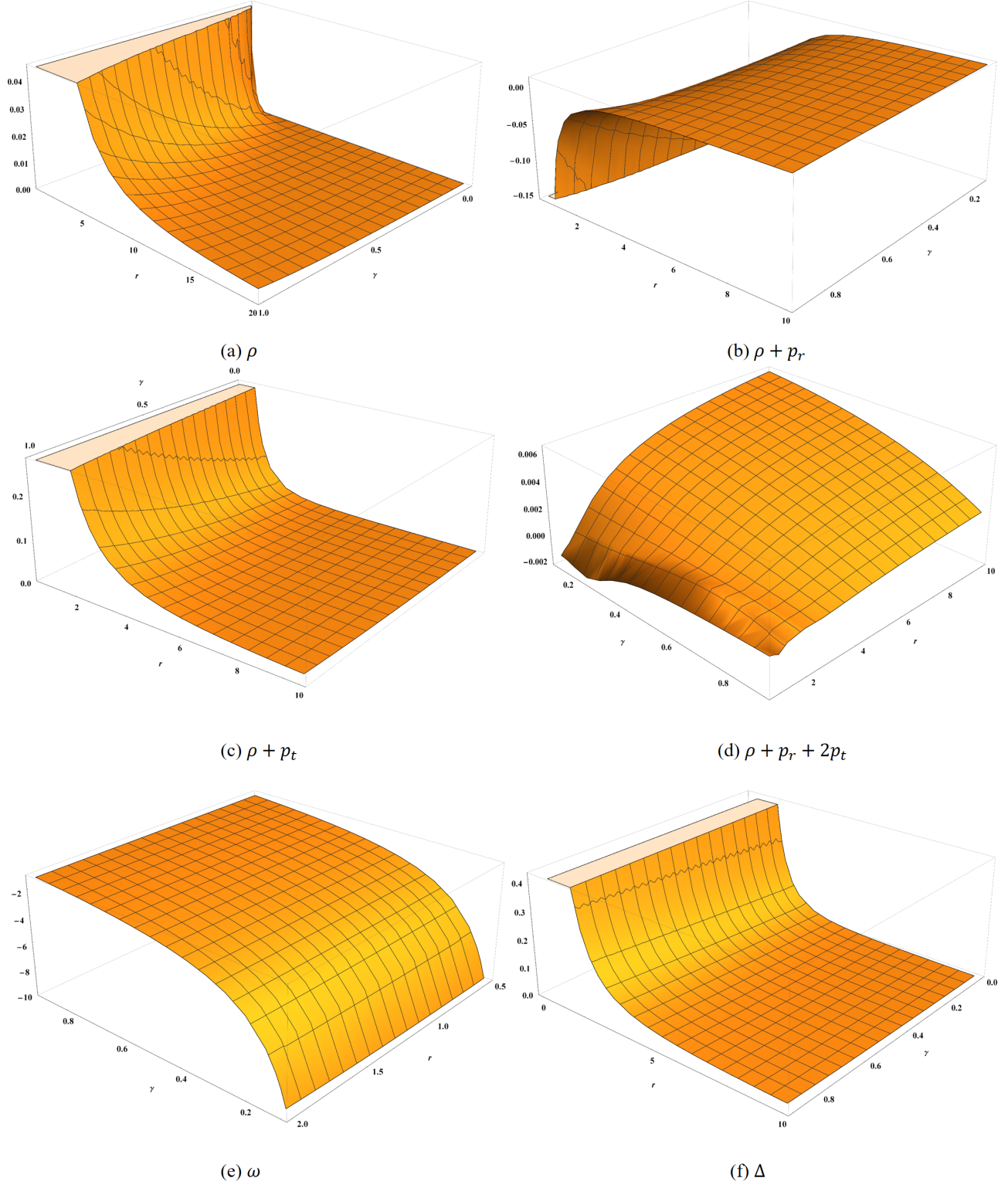


Figure 1: Plots of (a) ρ , (b) $\rho + p_r$, (c) $\rho + p_t$, and (d) $\rho + p_r + 2p_t$ for different combinations of model parameters in arbitrary units with $R_c = 1$ for Case I(a).

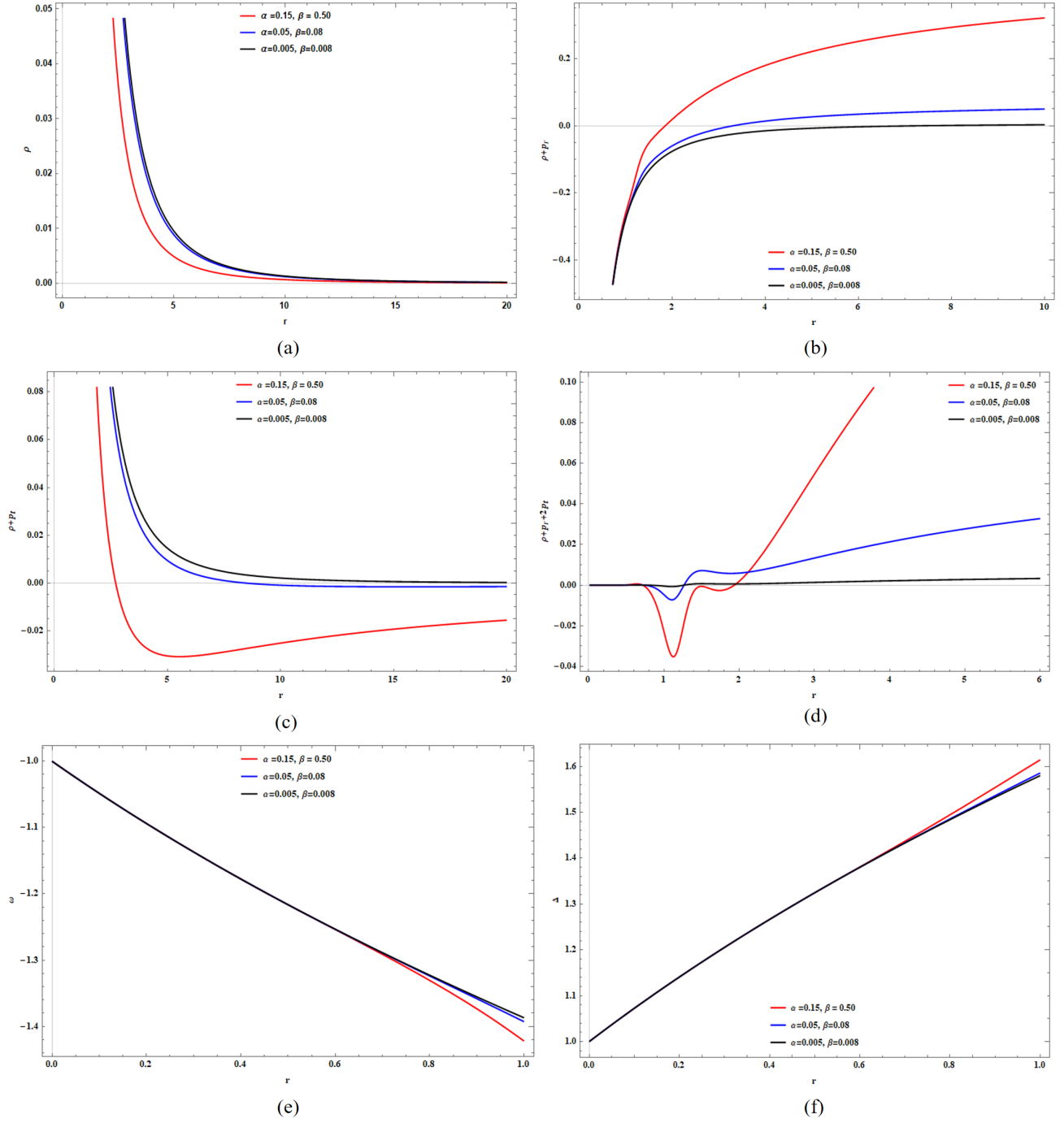


Figure 2: Plots of (a) ρ , (b) $\rho + p_r$, (c) $\rho + p_t$, and (d) $\rho + p_r + 2p_t$ for different combinations of model parameters in arbitrary units with $R_c = 1$ for Case I(b).

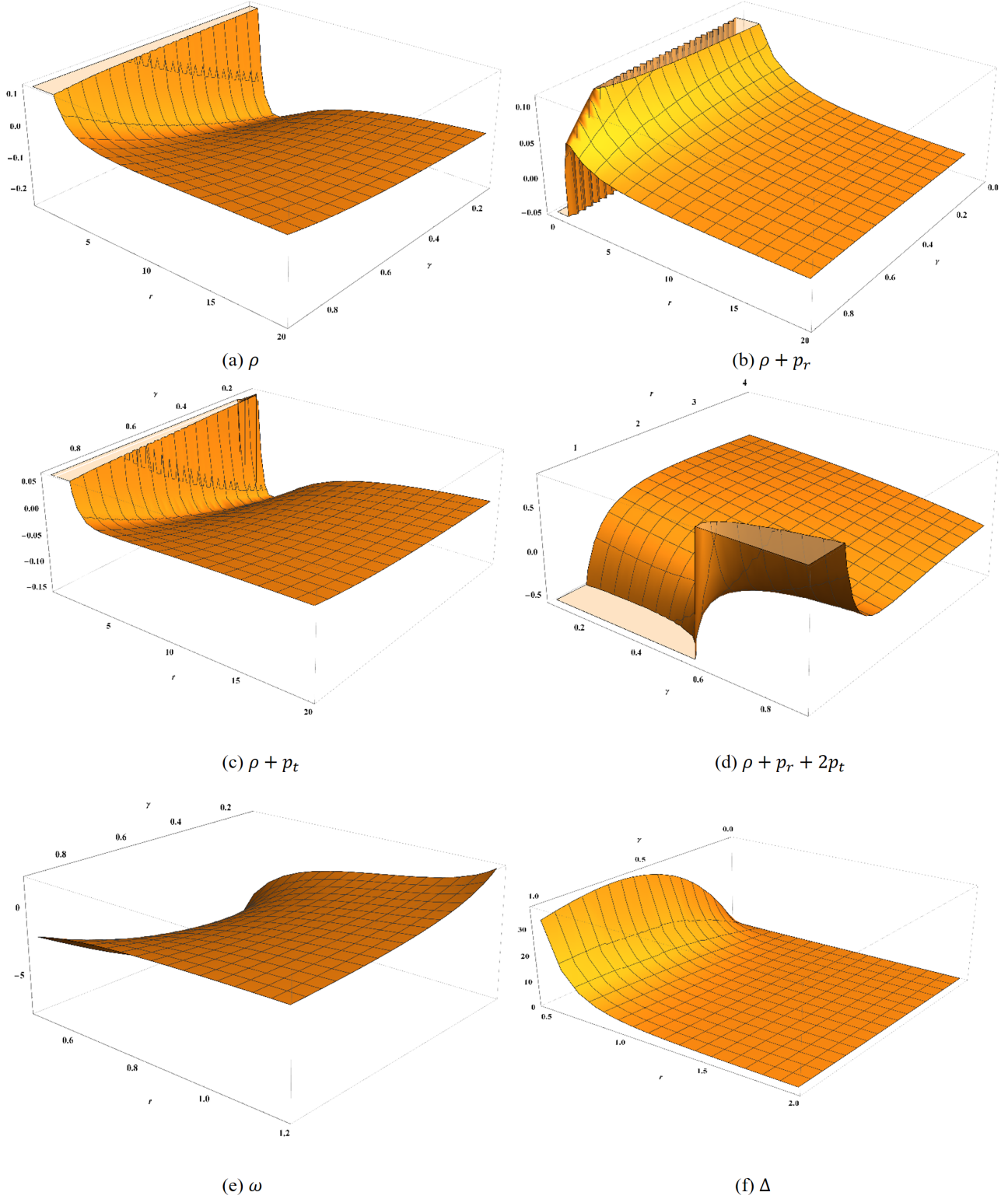


Figure 3: Plots of (a) ρ , (b) $\rho + p_r$, (c) $\rho + p_t$, and (d) $\rho + p_r + 2p_t$ for different combinations of model parameters in arbitrary units with $R_c = 1$ for Case II(a).

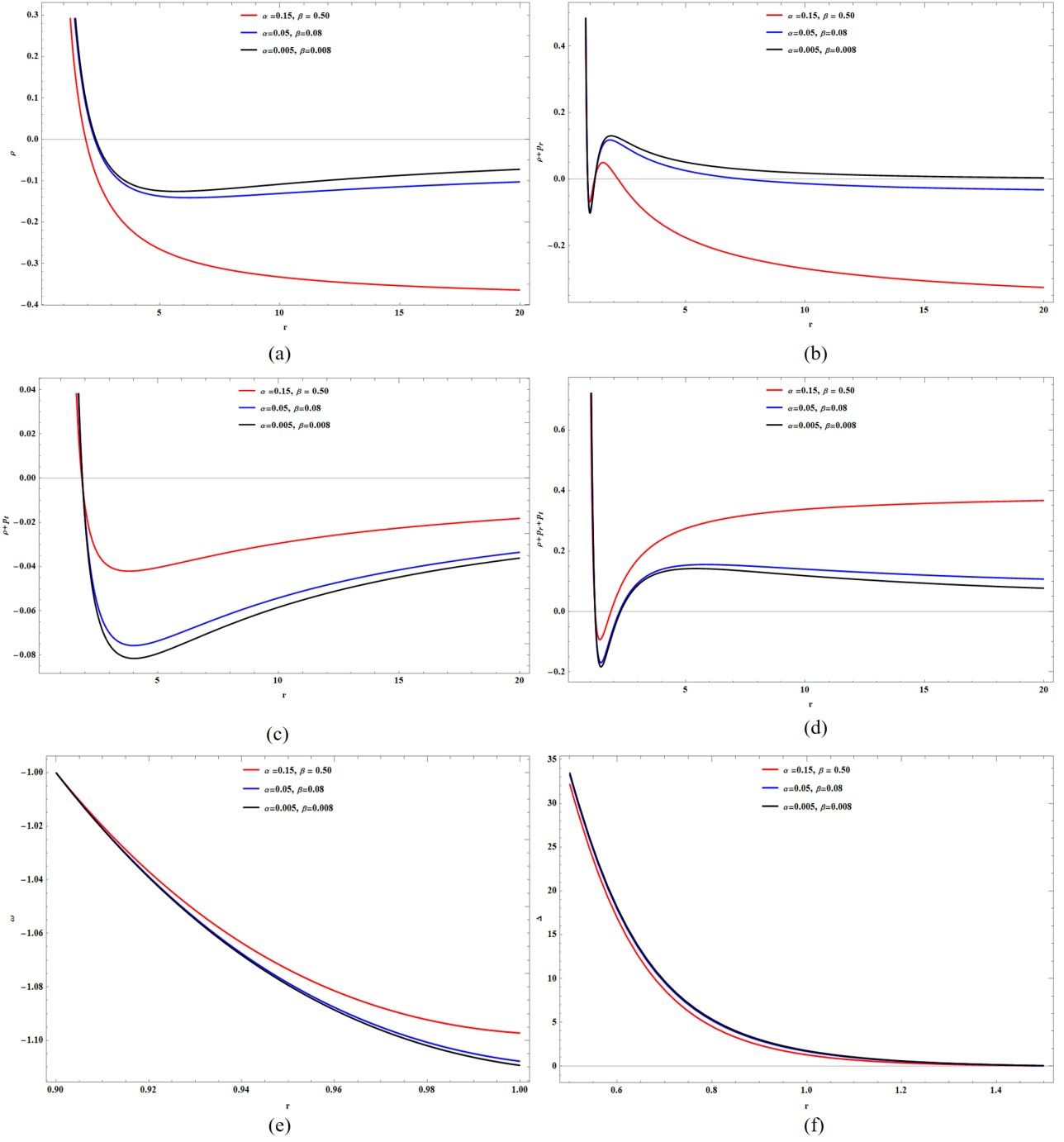


Figure 4: Plots of (a) ρ , (b) $\rho + p_r$, (c) $\rho + p_t$, and (d) $\rho + p_r + 2p_t$ for different combinations of model parameters in arbitrary units with $R_c = 1$ for Case II(b).

4 Discussions

The above analyses demonstrate that traversable wormholes can be realized in the $f(R)$ gravity model considered in this study. Especially, the results in **Case II(b)** are intriguing in that we obtain a phantom wormhole satisfying the energy conditions at the throat. Moreover, it is worth noting that we obtain a phantom-like profile of the source in all cases. Phantom wormholes satisfying the energy conditions in both GR and $f(R)$ gravity have been reported previously (for example in [31] and [32]), and these solutions have important implications. While $\omega < -1$ is an exotic phenomenon considering the Standard Model, it cannot be ruled out considering current cosmological observations. Intriguing properties of phantom energy include a long-range repulsive force [33] and the Big Rip mechanism in cosmology, which posits that the observable Universe should be ‘torn’ apart up to the smallest length scales in the infinite future due to the expansion driven by an EoS with $\omega < -1$. However, it has been shown that such scenarios can be avoided in certain models and by incorporating quantum corrections [34]. Moreover, non-trivial submicroscopic topologies may grow to macroscopic wormholes due to cosmic expansion [35]. An interesting candidate of phantom energy with a positive energy density as in our results is the *axion*, conventionally described by an antisymmetric rank-3 tensor field, and it is of significant interest in string theory and supergravity [36]. Wormholes supported by the axion field $f(R)$ gravity are issues to be addressed in a future report. Furthermore, we obtained a repulsive nature of the space-time geometries near the throat, which further support the anisotropic EoS in our results. Considering the fact that the major component of the observable Universe (dark energy) is described by an exotic EoS, the possibility of wormholes sustained by such sources cannot be ruled out.

In **Case I(b)**, we demonstrated that lower values of the model parameters α and β can restrict the need for exotic matter to small regions near the throat. This is an interesting feature considering the viability of the $f(R)$ gravity model at length scales comparable to that of the solar system, where GR has been verified extensively [37]. As demonstrated in the original work [28], decreasing the parameters α , β , and R_c can effectively make the model pass all local solar system tests. It is worth noting here that we have not considered conventionally derived arbitrarily small values of R_c to avoid loss of precision due to computational limitations. However, the choice of $R_c = 1$ is acceptable in that it does not violate condition $R/R_c > -1$, which ensures that the parameter be well-defined in the context of $f(R)$ theories [38]. In **Case I(a)**, we have considered a shape function originally proposed in [31], and checked the energy conditions in $f(R)$ gravity for the allowed range of the parameter γ . Our results show that a phantom wormhole solution is obtained with this combination of metric functions. However, in the $f(R)$ model considered here, we did not observe significant differences in energy condition violations depending on γ , contrary to analytical results in GR.

As discussed previously, the conventional approach of assuming a constant redshift function for computational simplicity may be an oversimplification. The redshift function can play a crucial role in determining energy condition violations, as apparent from Eqs. (18)-(20). In **Case II**, we presented results by assuming a simple functional form of the redshift function, and demonstrated that the energy conditions can be satisfied with a suitable combination of $\Phi(r)$ and $b(r)$. Using the shape function in Case I(b) and a simple redshift function, we obtained wormhole solutions with violations of energy conditions. In Case II(a), we used a logarithmic shape function with a simple redshift function to yield a wormhole respecting the energy conditions, which is the main highlight of our results. Some other combinations of adequate metric functions were also investigated, but the results were either physically unacceptable or not of particular interest in light of the previous analyses.

Furthermore, the violations of the energy conditions outside the wormhole throat for our solutions can be neglected, since the throat connecting two asymptotically flat regions is of primary concern in our analyses. Moreover, it is feasible to analytically cut off such solutions at some r_c away from the throat, and connect it to an exterior space-time at a junction interface with a cut-off of the stress-energy at r_c . Considering surface stress at the junction, a thin-shell is obtained around the wormhole (see for example [39]), and the junction acts as a boundary surface in the absence of surface stress. Physically, this approach corresponds to wormhole space-times in which some different stress-energy distribution becomes dominant at $r > r_c$.

5 Conclusions

In this study, we analyzed the energy conditions for Morris-Thorne-like wormhole solutions in a recently proposed $f(R)$ gravity theory. To the best of our knowledge, this is the first report on wormhole solutions in this particular $f(R)$ model. Moreover, we showed that traversable wormholes satisfying the energy conditions can be realized in this model with suitable choices of metric functions and model parameters. Although current observations do not yield evidence for wormholes in space-time, wormhole physics present important implications for fundamental issues

in gravity and the Standard Model. For example, wormholes may be leveraged to generate closed time-like curves that violate causality. Moreover, wormholes are connected to other fundamental issues such as the nature of the space-time foam, the $ER = EPR$ paradigm concerning quantum entanglement, the cosmic censorship conjecture, and non-trivial Euclidian space-time topologies in higher dimensional gravity. Another issues issue of significant research interest is the stability of wormhole solutions, and analytic wormhole solutions maybe obtained in this model for stability analyses against linear and nonlinear perturbations. Conventionally, the nonlinear field equations for spherically symmetric wormhole space-times are solved using suitable ansatzes for the metric functions. Although functional forms of $f(R)$ supporting wormholes maybe obtained using this approach, the resulting model obtained may not present stable de Sitter solutions or pass local solar system tests. To this end, our approach is advantageous in that we leverage a cosmologically viable $f(R)$ model with acceptable combinations of metric functions in our analyses. This approach may also be leveraged analytically to obtain non-trivial space-time configurations. These are open issues demanding further investigation. Furthermore, in addition to numerical and analytical wormhole solutions, potentially observable signatures of wormholes such as quasinormal modes and shadows are of significant interest in light of recent advances in VLBI techniques. These issues have not been addressed adequately in literature in the context of metric $f(R)$ gravity, and are subjects of future research.

References

- [1] M. Visser. *Lorentzian wormholes: From Einstein to Hawking*. Woodbury, USA, 1995.
- [2] M. S. Morris and K. S. Thorne. “Wormholes in space-time and their use for interstellar travel: A tool for teaching general relativity”. In: *Am. J. Phys.* 56 (1988), pp. 395–412.
- [3] T. Harko et al. “Modified-gravity wormholes without exotic matter”. In: *Phys. Rev. D* 87 (6 Mar. 2013), p. 067504.
- [4] F. S. N. Lobo and M. A. Oliveira. “Wormhole geometries in $f(R)$ modified theories of gravity”. In: *Phys. Rev. D* 80 (10 Nov. 2009), p. 104012.
- [5] A. DeBenedictis and D. Horvat. “On wormhole throats in $f(R)$ gravity theory”. In: *General Relativity and Gravitation* 44.11 (2012), pp. 2711–2744.
- [6] N. Furey and A. DeBenedictis. “Wormhole throats in R^m gravity”. In: *Classical and Quantum Gravity* 22.2 (Dec. 2004), pp. 313–322.
- [7] A. De Felice and S. Tsujikawa. “ $f(R)$ Theories”. In: *Living Reviews in Relativity* 13.1 (June 2010).
- [8] S. Nojiri and S. D. Odintsov. “Introduction to modified gravity and gravitational alternative for dark energy”. In: *International Journal of Geometric Methods in Modern Physics* 04.01 (Feb. 2007), pp. 115–145. ISSN: 1793-6977.
- [9] A. A. Starobinskiĭ. “Spectrum of relic gravitational radiation and the early state of the universe”. In: *Soviet Journal of Experimental and Theoretical Physics Letters* 30 (Dec. 1979), p. 682.
- [10] A.A. Starobinsky. “A new type of isotropic cosmological models without singularity”. In: *Physics Letters B* 91.1 (1980), pp. 99–102.
- [11] A. A. Starobinsky. “Disappearing cosmological constant in $f(R)$ gravity”. In: *JETP Letters* 86.3 (Oct. 2007), pp. 157–163.
- [12] W. Hu and I. Sawicki. “Models of $f(R)$ cosmic acceleration that evade solar system tests”. In: *Physical Review D* 76.6 (Sept. 2007).
- [13] S. Tsujikawa. “Observational signatures of $f(R)$ dark energy models that satisfy cosmological and local gravity constraints”. In: *Physical Review D* 77.2 (Jan. 2008).
- [14] T. Katsuragawa et al. “Gravitational waves in $f(R)$ gravity: Scalar waves and the chameleon mechanism”. In: *Physical Review D* 99.12 (June 2019).
- [15] T. Katsuragawa et al. “Gravitational waves in $f(R)$ gravity: Scalar waves and the chameleon mechanism”. In: *Physical Review D* 99.12 (June 2019).
- [16] N. Godani and G. C. Samanta. “Traversable wormholes and energy conditions with two different shape functions in $f(R)$ gravity”. In: *International Journal of Modern Physics D* 28.02 (Jan. 2019), p. 1950039.

- [17] G. C. Samanta and N. Godani. “Wormhole modeling supported by non-exotic matter”. In: *Modern Physics Letters A* 34.28 (Sept. 2019), p. 1950224.
- [18] G. C. Samanta and N. Godani. “Validation of energy conditions in wormhole geometry within viable $f(R)$ gravity”. In: *The European Physical Journal C* 79 (July 2019).
- [19] N. Godani and G. C. Samanta. “Static traversable wormholes in $f(R, T) = R + 2\alpha \ln T$ gravity”. In: *Chinese Journal of Physics* 62 (Dec. 2019), pp. 161–171.
- [20] N. Godani and G. C. Samanta. “Non violation of energy conditions in wormholes modeling”. In: *Modern Physics Letters A* 34.28 (2019), p. 1950226.
- [21] G. C. Samanta, N. Godani, and K. Bamba. “Traversable wormholes with exponential shape function in modified gravity and general relativity: A comparative study”. In: *International Journal of Modern Physics D* 29.09 (2020), p. 2050068.
- [22] N. Godani and G. C. Samanta. “Traversable wormholes in $R + \alpha R^n$ gravity”. In: *The European Physical Journal C* 80 (Jan. 2020).
- [23] N. Godani and G. C. Samanta. “Traversable wormholes in $f(R)$ gravity with constant and variable redshift functions”. In: *New Astronomy* 80 (Oct. 2020), p. 101399.
- [24] N. Godani and G. C. Samanta. “Wormhole modeling in R^2 gravity with linear trace term”. In: *International Journal of Modern Physics A* 35.08 (Mar. 2020), p. 2050045.
- [25] S. Habib Mazharimousavi and M. Halilsoy. “Wormhole solutions in $f(R)$ gravity satisfying energy conditions”. In: *Modern Physics Letters A* 31.34 (2016), p. 1650192.
- [26] H. Saiedi and B. Nasr Esfahani. “Time-dependent wormhole solutions of $f(R)$ theory of gravity and energy conditions”. In: *Modern Physics Letters A* 26.16 (2011), pp. 1211–1219.
- [27] G. Cognola et al. “Class of viable modified $f(R)$ gravities describing inflation and the onset of accelerated expansion”. In: *Phys. Rev. D* 77 (4 Feb. 2008), p. 046009.
- [28] D. J. Gogoi and U. Dev Goswami. “A new $f(R)$ gravity model and properties of gravitational waves in it”. In: *Eur. Phys. J. C* 80.12 (2020), p. 1101.
- [29] L. Boubekeur et al. “Current status of modified gravity”. In: *Phys. Rev. D* 90 (10 Nov. 2014).
- [30] F. S. N. Lobo, F. Parsaei, and N. Riazi. “New asymptotically flat phantom wormhole solutions”. In: *Phys. Rev. D* 87 (8 Apr. 2013), p. 084030.
- [31] Francisco S. N. Lobo. “Phantom energy traversable wormholes”. In: *Phys. Rev. D* 71 (8 Apr. 2005), p. 084011.
- [32] P. Pavlovic and M. Sossich. “Wormholes in viable $f(R)$ modified theories of gravity and weak energy condition”. In: *The European Physical Journal C* 75.3 (Mar. 2015). ISSN: 1434-6052.
- [33] L. Amendola. “Phantom Energy Mediates a Long-Range Repulsive Force”. In: *Physical Review Letters* 93.18 (Oct. 2004). ISSN: 1079-7114.
- [34] E. Elizalde, S. Nojiri, and S. D. Odintsov. “Late-time cosmology in a (phantom) scalar-tensor theory: Dark energy and the cosmic speed-up”. In: *Physical Review D* 70.4 (Aug. 2004). ISSN: 1550-2368.
- [35] Thomas A. Roman. “Inflating Lorentzian wormholes”. In: *Phys. Rev. D* 47 (4 1993), pp. 1370–1379.
- [36] J. E. Kim. “A Theoretical Review of Axion”. In: *COSMO-99* (Sept. 2000).
- [37] J-Q Guo. “Solar System tests of $f(R)$ Gravity”. In: *International Journal of Modern Physics D* 23.04 (Mar. 2014), p. 1450036. ISSN: 1793-6594.
- [38] L. Amendola and S. Tsujikawa. *Dark energy: theory and observations*. Cambridge University Press, 2010.
- [39] E. F. Eiroa and G. F. Aguirre. “Thin-shell wormholes with charge in $F(R)$ gravity”. In: *The European Physical Journal C* 76.3 (Mar. 2016). ISSN: 1434-6052.